The FANTASIO+ set-up to investigate jet-cooled molecules: Focus on overtone bands of the acetylene dimer.

Keevin Didriche, Clement Lauzin, Tomas Foldes, Xavier de Ghellinck d'Elseghem Vaernewijck, Michel Herman

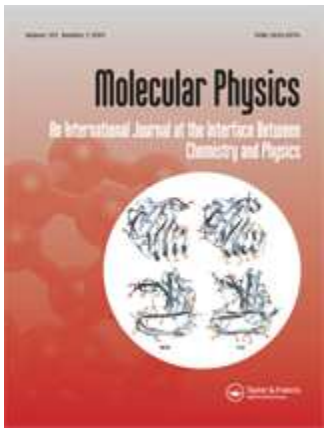

The FANTASIO+ set-up to investigate jet-cooled molecules: Focus on overtone bands of the acetylene dimer.

Journal:	*Molecular Physics*
Manuscript ID:	TMPH-2010-0115
Manuscript Type:	Special Issue Paper - Solvay workshop
Date Submitted by the Author:	02-Apr-2010
Complete List of Authors:	Didriche, Keevin; Université Libre de Bruxelles, Chimie quantique et Photophysique LAUZIN, Clement; Université Libre de Bruxelles, Chimie quantique et Photophysique FOLDES, Tomas; Université Libre de Bruxelles, Chimie quantique et Photophysique de Ghellinck D'Elseghem Vaernewijck, Xavier; Université Libre de Bruxelles, Chimie quantique et Photophysique Herman, Michel; Université Libre de Bruxelles, Chimie quantique et Photophysique
Keywords:	van der Waals complexe, acetylene dimer, acetylene-argon dimer, CW-CRDS, overtone spectra in molecular complexes

The FANTASIO+ set-up to investigate jet-cooled molecules: Focus on overtone bands of the acetylene dimer.

K. Didriche[a], C. Lauzin, T. Földes[b], X. de Ghellinck D'Elseghem Vaernewijck[c], and M. Herman.

Laboratoire de Chimie quantique et Photophysique

Faculté des Sciences

CP160/09

Université libre de Bruxelles

Ave. Roosevelt, 50

B-1050

Brussels, Belgium

[a] Postdoctoral Researcher (F.R.S.-FNRS)

[b] ARC postdoctoral researcher

[c] FRIA Researcher

Pages: 30

Figures: 6

Tables: 2

Send mail to M. Herman
Email: mherman@ulb.ac.be

Abstract

The experimental set-up FANTASIO, for "Fourier trANsform, Tunable diode and quadrupole mAss spectrometers interfaced to a Supersonic expansIOn" (M. Herman, K. Didriche, D. Hurtmans, B. Kizil, P. Macko, A. Rizopoulos, and P. Van Poucke, Mol. Phys. **105**, 815 (2007)) built in Brussels has been updated. The turbomolecular pumping system of the supersonic expansion has been doubled and new mirrors, with reflectivity 99.999% instead of 99.99%, have been set in the CW-cavity ring down spectrometer (CW-CRDS) probing jet-cooled molecules. The changes all together result in a signal to noise increased by up to a factor 10, around 1.5 μm. These improvements are demonstrated with various acetylene data in the 2CH excitation range, including the assignment of a new sub-band of acetylene-Ar, with K'-K" = 2-3. The focus is set on the acetylene dimer. Overtone sub-bands, with *b*- and *a*-type structures, are identified for the first time in the literature. The former are assigned to vibrational excitation in the hat unit of the T-shaped dimer, the latter, tentatively, to vibrational excitation in both units. The relevance of the overtone data on acetylene dimers for space remote sensing is highlighted.

I. Introduction

A vast experimental and theoretical literature was published mainly in the 90's about acetylene multimers (see *e.g.* [1 2 3 4 5 6 7 8 9 10 11 12 13 14 15 11 16 17 18 19 20 21 22 23 24 25 26 27 28 29 30 31 32 33 34 35 36]). As a rule, the transition dipole moments in van der Waals complexes mainly arise from the monomer units and the bands in the complexes usually lie very close to strong monomer bands. Acetylene multimers were reported around two infrared bands in the monomer: ν_5, the *cis*-bending at 730 cm^{-1} and ν_3, the CH asymmetric stretch at 3300 cm^{-1}. Overtone bands in pure acetylene multimers were so far not reported. Following a preliminary low resolution report for acetylene-Ar[37], overtone bands in mixed dimers containing acetylene were recently detected in a supersonic expansion, under sub Doppler conditions. These dimers are of acetylene with Ar[38], CO_2[39] and N_2O[40]. The related acetylene monomer transition is $\nu_1+\nu_3$ (with ν_1 the symmetric CH stretch), with origin at 6556.46 cm^{-1} [41 42]. It will be further referred to here as 2CH excitation. These experiments were performed in Brussels using the FANTASIO set-up (for "Fourier trANsform, Tunable diode and quadrupole mAss spectrometers interfaced to a Supersonic expansIOn"). CW-cavity ring down spectroscopy (CW-CRDS)[43 44 45] was the detection technique.

While recording acetylene-Ar, other, larger absorption features were observed in the spectra. Contrary to all three assigned acetylene-Ar sub-bands in the range investigated which show resolved structure[38], only few of these absorption features showed separate lines or clumps of lines. One of them was tentatively attributed to the pure acetylene dimer[46]. Other broader spectral features have not been reported in the literature, yet. Further evidence was brought for the formation of acetylene multimers in the expansion from very specific monomer line profiles. Indeed a central dip appears in the acetylene monomer line profile when using axisymmetric nozzles. These dips were observed in both acetylene-Ar and pure acetylene expansions. They were attributed to the decrease in monomer absorption due to condensation in the central part of the conical expansion, among other reasons [46] [47].

We have since modified FANTASIO. The pumping efficiency has been improved and higher performance mirrors have been installed in the CW-CRDS spectrometer. These changes are presented and illustrated in section II. The resulting set-up, named FANTASIO+ has been used to record new spectra using acetylene seeded in various rare gas expansions. The experimental results presented in section III are exploited to assign the carriers of the broad spectral features to acetylene multimers. These are identified and the bands are assigned in section IV. The results are discussed and put in the perspective of remote sensing in section V, before concluding.

II. FANTASIO+

FANTASIO was described previously in the literature[48]. Relevant to the present investigation are the CW-CRDS spectrometer and the supersonic expansion. Only their main features are recalled in this section, and the changes highlighted. The reader should note that the detailed experimental conditions for the spectra that will be presented are indicated in the figure captions and not detailed in the text. Acetylene was from Air Liquide (99.6 % purity) and used without further purification. The many strong lines from the monomer ($^{12}C_2H_2$ or $^{12}CH^{13}CH$) appearing on the spectra are not identified in the Figures.

A. Supersonic expansion

In the new set-up, named FANTASIO**+**, the free supersonic jet expansion is produced using two identical, large turbomolecular pumps (Leybold MAG W3200 CT; 3200 l/s). They are teflon coated and backed by an Alcatel ADS 860 HII group. The previous system had only one of these, with the same primary pumps. Both turbomolecular units are directly mounted below the cylindrical expansion cell, about 32 cm in diameter. The Y connection matches the identical pump and cell diameters. The reservoir (p_0) and residual (p_∞) pressures are measured using MKS Baratron gauges (1000 and 1 torr full scale, respectively). The acetylene and carrier gas flows are measured using MKS and Brooks flowmeters (10000 and 50000 sccm

full scale, respectively –SCCM denotes cubic centimeter per minute at STP). The reservoir pressure is now typically 100 kPa, as opposed to 50 kPa before, for similar residual pressures, of the order of 1 Pa. Thanks to the increased pressure ratio and flow rates, the signal to noise ratio (S/N) is boosted. This is illustrated in Figure 1. Spectra of C_2H_2-Ar recorded with one and two turbomolecular pumping units are shown in panels (1) and (2), respectively. The comparison demonstrates an increase of a factor 2 in the S/N. As another consequence, He and Ne could be used as carrier gases, in addition to Ar, while overriding the pump capacity before. A wider range of experimental degrees of freedom is thus made available. This will be exploited in section III.

B. CW-CRDS spectrometer

The general features of the CW-CRDS spectrometer, directly inspired by the developments from Romanini and coworkers[49 50], are unchanged in FANTASIO+. DFB tunable diode lasers (TDL) emitting in the 1.5 μm range (e.g. ILX lightwave, 1 MHz linewidth) are used. The TDL beam is sent through an optical isolator (Thorlabs 4015 5AFC-APC) and then split by a coupler (Thorlabs, 10 202A-99-APC). Some 1% of the light intensity is sent via a fiber collimation package (f=8 mm) into a home-made Fabry-Pérot interferometer made of two 50% reflectivity flat mirrors positioned on an Invar bar. This etalon provides a FSR of about 955 MHz. The remaining 99% of the light is focused by a fiber collimation package (f=4.5 mm) onto

an acousto-optical modulator (AOM) from AA Opto-Electronic (MGAS 80-A1). The first order diffraction from the AOM is injected into the TEM_{00} mode of a linear ring-down cavity through two lenses (f_1=30 mm, f_2=50 mm) and two steering mirrors. The cavity is composed of two concave mirrors (Radius = 1000 mm), separated by about 540 mm. The output mirror is mounted on a piezo actuator (Piezomechanik HPST 1000/15-8/5). The light exiting the cavity is focused through a lens (f=20 mm) on a photodiode. The light detection system from FANTASIO was modified and is described later in this section.

For ring-down detection, the piezo actuator is driven at a selected frequency (typically 500 Hz) and cavity mode matching with the laser is achieved at twice the selected frequency. The AOM is switched off as soon as the cavity mode intensity attains a threshold value. The same event triggers the measurement procedure of the ring-down decay. This procedure is controlled by the same home-made electronics as before. The ring-down decays are sampled by a PCI-6251 multifunction data acquisition card, with 16bit 1.25 MHz analog-to-digital converter. The acquisition is PC driven by home-made software written using LabVIEW. Each ring-down exponential decay is fitted by a procedure based on the nonlinear Levenberg-Marquardt method. The absorption coefficient α is directly calculated using [44]:

$$\alpha = (\nu - \nu_0)\frac{L}{cl} \qquad (1)$$

in which ν_0 is the ring-down decay frequency in an empty cavity (*i.e.* without absorber), L and l are respectively the lengths of the cavity and the absorption path in the medium and c is the speed of light. The TDL frequency can be continuously tuned by sweeping the temperature using a home-made PID stabilizer. The temperature tuning from about 60 °C to –5 °C corresponds approximately to the 6534 to 6570 cm^{-1} spectral range when using the diode mentioned earlier.

The most significant difference from FANTASIO is the typical ring-down time. It was between 15 and 20 μs in our previous experiments. It has been increased to some 120 μs, using a new set of mirrors (Layertec). Their measured reflectivity is R = 99.9985%. The number of passes has been extended from about 8300, previously, to 66000 now. When using a slit 1 cm long (and 30 μm wide), as in the present version of FANTASIO**+**, the effective absorption path in the cooled gas is 660 m.

As an effect of the very high reflectivity of the new cavity mirrors the typical light power leaking out of the cavity has significantly decreased. A new detection system comprising a Hamamatsu InGaAs PIN photodiode (G8376-03) connected in photoconductive mode with a three-stage readout circuit is employed to record ring-down transients reliably. In the readout circuit a JFET-input stage operational amplifier (OPA657) connected as a wideband transimpedance amplifier is used. The second stage amplifier (OPA843) provides additional adjustable gain and offset. A

fully-differential amplifier (THS4503) for single-ended to differential conversion drives the analog-to-digital converter. Low-pass filtering is set so that 1 μs small-signal pulses can be satisfactorily resolved. Careful attention has been given to circuit-board layout to minimize leakage current and parasitics.

As an illustration of the results, the spectrum in panel (3) in Figure 1 was recorded using the updated spectrometer, in addition to the two pumps used for panel (2). Spectra in Figure 1 were recorded at different stages of the development of the set-up. The slit length and therefore the flow rates, in particular, were modified. Accounting for these variations, the S/N is improved by a factor of about 5 between panels (2) and (3). The intensity scale was multiplied by the required factor (1.5) in panel (3), to achieve comparable visual noise level to panel (2). The gain from the pump doubling, demonstrated from panel (1) to (2), was about 2. The overall gain in S/N between FANTASIO and FANTASIO**+**, comparing regular operational conditions, is thus about 10. The present α_{min}, approximated as S/N = 2/1 and calculated for 1 cm absorption path under the slit nozzle, is calculated to be 3.18 10^{-8} cm^{-1}. This significant improvement will be fully exploited when getting to the detailed rotational analysis of the spectral features. This step is, however not achieved in this investigation, yet.

III. Experimental results

The spectral range of interest to the present investigation is from 6534 to 6565 cm^{-1}. Thanks to the increased pumping capacity, acetylene spectra could be recorded using various carrier gases and nozzle geometries. This is illustrated in Figure 2. The spectrum in the middle panel was recorded with Ar and a slit nozzle. The one in the top panel was recorded using Ne and an axisymmetric nozzle. As pointed out in the previous section, the use of Ne was previously limited by the single pump capacity. Despite the double pumping scheme, a circular nozzle of reduced diameter (150 microns) had still to be used when recording the spectrum with Ne. The comparison in Figure 2 demonstrates that numerous spectral features are observed independently of the carrier gas. They can therefore reliably be assigned to acetylene multimers. Their appearance may actually vary from one carrier gas and nozzle type to another because of different cooling conditions. These bands, listed in Table 1, thus provide definite evidence for the existence of pure acetylene weakly bound molecular complexes in the overtone spectral range.

Multimer production using FANTASIO**+** appears to be optimal when using Ar as a carrier gas, compared to Ne and He. Unfortunately, acetylene-Ar bands are also strong and new sub-bands compared to our previous report[38] are observed on the spectra recorded using FANTASIO**+**. They are often overlapped with multimer bands creating severe identification problems whenever focusing on more structured spectral features, in particular.

We attempted to discriminate the molecular carrier of the bands by varying the experimental conditions. The related spectra were actually recorded using the

two pumping units before the new CW-CRDS system was installed. They nevertheless provide the relevant information and are used in this section. A spectral range showing only previously unidentified absorption features is selected in Figure 3. The amount of carrier gas (Ar) was kept constant while changing the flow of acetylene by up to a factor 3, from bottom to top in this Figure. For some of the features, including most of the well resolved lines, the intensity decreases when adding acetylene. This response to experimental changes is found to characterize all known acetylene-Ar sub-bands. This is illustrated with the known K'-K" = 2-1 sub-band[38] in Figure 4, which shows another section of the same three sets of spectra presented in Figure 3. Most of the resolved features in Figure 3 are thus from acetylene-Ar. They turn out to be the K'-K" = 2-3 sub-band, not previously reported, with the *P* branch forming the band head at 6548.417 cm^{-1} and the *Q* branch starting at 6548.792 cm^{-1}. The upper K' = 2 sub-state was already observed through the 2-1 sub-band and found to be perturbed[38]. Band simulations not further detailed here demonstrate that the lower K" = 3 sub-state, not previously reported, is also perturbed as could be predicted from literature results concerning K" =2 [51]. A more detailed analysis of the acetylene-Ar sub-bands revealed by FANTASIO+ is under way and not further detailed in this report.

The trend when varying pressure conditions is different for other spectral features such as the broad absorption at 6546.5 cm^{-1} appearing in Figure 3. The band intensity indeed increases when doubling the acetylene flow rate. We checked that this other behavior characterizes all bands listed in Table 1 that could

be assigned to acetylene multimers. It is interesting to notice that the growing of the multimer bands with increasing acetylene flow rate stops when tripling the acetylene concentration, as shown in the top panel of Figure 3. This trend probably corresponds to the decrease in cooling efficiency and therefore in multimer production. The final experimental conditions were accordingly adapted and fine tuned, depending if investigating acetylene-Ar or acetylene multimers.

The present comparison provides more detailed insight than the one between Ne and Ar carrier gases in Figure 2. It can *e.g.* be checked that weaker resolved lines and unresolved clumps appearing in the middle of the acetylene-Ar sub-band in Figure 3 between 6548.4 and 6549.0 cm^{-1}, are behaving similarly as the broad feature at 6546.5 cm^{-1}. Their carrier is thus identified to an acetylene multimer.

IV.Assignment of multimer bands

We focus now on the multimer spectral features. We attempted various simulations using literature constants for the dimer[52], trimer[9 14] and tetramer[14]. Colin Western's PGOPHER program[53] was used. Although reasonable match could be achieved for specific bands with the larger aggregates constants, none agreed as well as the one presented in Figure 2, at the bottom. This simulation uses *b*-type selection rules, involving an upper state of B_2 symmetry, for a rigid T-shaped structure in a C_{2v} group symmetry. The comparison definitely identifies the pure

acetylene dimer as the carrier. The match is impressive, accounting for almost all sub-bands assigned to multimers. These are identified using the conventional ${}^{\Delta K}\Delta J_{K''}(J'')$ notation in both Figure 2 and Table 1. We did not include tunneling effects[11] in the simulation. We only accounted for the 1:3 intensity alternation expected for a rigid-type molecule. Previous investigation of mixed acetylene dimers, with CO_2[39], N_2O[40] and Ar[38], demonstrated extensive perturbations in this 2CH excitation range. They are further confirmed with the K'-K" = 2-3 sub-band in acetylene-Ar briefly discussed in the previous section. For the pure dimer, one can check in Figure 2 that several of the sub-band origins are not properly reproduced. More detailed comparisons confirm the existence of perturbations compared to rigid-asymmetric top-type predictions. The detailed analysis of the overtone pure acetylene dimer bands will require a dedicated investigation. The constants used for the simulation, listed in Table 2, are thus approximate and preliminary. Those of the ground state in this Table correspond to the mean value of the three sets published in their Table VI by Fraser and coworkers[11]. Only the most influent parameters on the band contour simulation were considered. The upper state constants were adjusted empirically for optimal match with the various broader dimer structures.

One additional broader feature is apparent in Figure 2, with prominent *Q* and *R* branches around 6538.3 and 6539.5 cm^{-1}, respectively. It is not accounted for in the simulation of the dimer structure just discussed. We first checked that $\nu_1+\nu_3$ was the only band in the monomer in the range investigated. We then attempted

simulations of the observed band contour using rotational constants based on ground state rotational constants. We again started with trimer and the tetramer literature constants. Reasonable match could be achieved in both cases. But, again, the comparison with the dimer was strikingly convincing. It is presented in Figure 5 (top). This time, however, *a*-type selection rules are required in the simulation, involving an upper state of A_1 symmetry. The upper state constants obtained similarly as for the *b*-type band are listed in Table 2. To optimize the comparison, *a*- and *b*-type structures contributing to the spectral features in the range covered in Figure 5 were overlapped (middle). The *b*-type ${}^{p}Q_3(J)$ sub-band, already mentioned to be perturbed, were red-shifted by 0.34 cm^{-1} in the simulation to improve the agreement. The same shift was applied to the weaker ${}^{p}Q_4(J)$ and ${}^{p}Q_5(J)$ subbands. Only the ${}^{p}Q_3(J)$ sub-band is visible among the *a*-type absorption feature.

V. Discussion

The dimer is known to be planar, T shaped [10 52], thus with perpendicular "hat" and "body" acetylene monomer units. We shall hereafter label these units 1 and 2, respectively, as indicated in Figure 6. The *b*-type structure we have reported in the pure dimer, which was simulated in Figure 2, is typical of all acetylene mixed dimers[38 39 40]. The 2CH excitation ($\nu_1+\nu_3$ in the monomer) is along the *b*-axis of inertia that is located in unit 1 for the pure dimer.

The origin of the *a*-type band (6538.3 cm^{-1}), which only occurs in the pure dimer, is red-shifted compared to the *b*-type one by about 8 cm^{-1} (6547.6 cm^{-1}). The same shift was found to occur in the 3 μm, 1CH (ν_3) band between the similar *a*- and *b*-type excitation bands[11]. It is likely to be due for both 1CH and 2CH excitations to the encaged nature of the C-H bond of unit 2 making the van der Waals bond with unit 1 (see Figure 6). The movement of this CH bond is restricted and the vibrational frequency is reduced. If correct, this statement should also apply to the other, symmetric CH vibration, *i.e.* ν_1 in the monomer. Such a reduction in both CH fundamentals is predicted by *ab initio* calculations[10]. So, if the 2CH *a*-type excitation entirely occurred in unit 2, one should expect the *a*-type band origin to be red-shifted compared to the *b*-type one by roughly twice as much as for ν_3 in the 1CH range, *i.e.* about 16 cm^{-1}. Since shifts are almost identical, *i.e.* about 8 cm^{-1}, it looks as if the 2CH excitation giving rise to the *a*-type band occurred in different acetylene units. The asymmetric CH excitation (similar to ν_3 in the monomer) takes place in unit 2; it is responsible for the band strength and selection rules. The symmetric excitation (similar to ν_1 in the monomer) occurs in unit 1; it presents the same frequency parameters as in the other, *b*-type excitation. This explanation, however, does not account for any possible change in x_{13}, the mixed anharmonicity parameter. Nor does it account for any modification in the strength of anharmonic resonances in monomer and dimer structures, also responsible for the values of the band origins. Unfortunately, the rotational constants listed in Table 2 are not very helpful in this problem. As for ν_3 [11], indeed, the asymmetric top rigid-type Hamiltonian we have

used is not adequate and the upper state rotational constants cannot be reliably compared. The present assignment in terms of mixed excitation in the two acetylene units is only based on the shift of the vibrational band origins. It remains tentative. If ever confirmed, it would probably be the first such case to be reported, for any van der Waals dimer.

The present results account for the multimer bands revealed thanks to the increased performances of FANTASIO+. Aggregates larger than the dimer seem therefore not to be observed on the spectra we have recorded. Much larger pressure ratios p_0/p. were usually associated to their observation in the lower IR region in the literature, usually with He as carrier gas and sometimes with pulsed injection systems. Nevertheless, we were able to observe larger multimers with the previous FANTASIO set-up around 3 μm using Ar^{35}, thus before adding the second turbomolecular pump. Their absence could therefore indicate their fast predissociation in the presently investigated, 2CH excitation range. This is thus not the case with dimers.

The optimal temperature for the simulations was found to be T_{rot} = 20 K. Lines from all relevant J/K states were included in the simulation. We convolved the Doppler line profile for T_{rot} = 20 K with a Lorentzian profile. The optimal FWHM was found to be 0.015 and 0.075 cm^{-1} for *b*- and *a*-type transitions, respectively. These values are much larger than for acetylene-Ar in the same range. In this mixed dimer, the widths for unperturbed lines were determined to be 7 10^{-4} cm^{-1} FWHM, corresponding to a mean half-time of 7.5 ns[38]. The wider profiles in the pure dimer

indicate a much smaller lifetime. It is even five times shorter in the A_1 upper state, corresponding to vibrational excitation in unit 2, than in the B_2 state involving unit 1 excitation. However, the present values result from the analysis of band contours with strong line overlap. They need to be confirmed from a detailed line analysis. In any case, the present results demonstrate that this problem does not prevent the pure dimer species to be monitored and detected *in situ*, around 1.5 μm.

Acetylene is observed in numerous outer environments such as comets[54 55 56], planetary [57 58] (including Earth[59 60] and Titan[61]) and stellar[62 63 64] atmospheres, and the interstellar medium[65 66 67 68 69]. Some of the laboratory experiments[6 20] report the observation of acetylene dimers under temperature conditions are not that different from those on Titan for instance. Furthermore, pressure conditions in some outer environments such as Titan are in favor of the formation of aggregates, as specifically investigated in [20]. It is therefore not unlikely that acetylene dimers be formed in space.

Portable spectrometers are nowadays becoming available in the NIR spectral range[70 71], often providing significantly increased sensitivity compared to mid IR remote sensors. The telecom DFB diode laser spectral range, around 1.6 μm, as presently used, is of specific relevance for space detection. These lasers are fibered, portable and can indeed be associated to ultra high sensitivity techniques as the one used in the present investigation. This increased detection sensitivity, compared to typical FTIR sensors compensates for the smaller band strength of overtone and combination bands in the NIR region, compared to fundamental bands in the lower

IR. In addition, thanks to increased contribution of anharmoncity parameters, the stronger overtone vibrational bands, involving multiple CH excitation for instance, are usually more separated from one species to another in the overtone range, thus decreasing overlapping problems and making the band search easier. Finally, we have now demonstrated that pure acetylene dimers can be observed and spectroscopically characterized at high vibrational excitation energies, around 2CH stretches. The NIR region therefore provides an appealing alternative for remote sensing of the pure acetylene dimers in space.

VI.Conclusion

The FANTASIO set-up developed in Brussels was modified by including a second turbomolecular unit to produce the expansion. As a result, carrier gases other than Ar could be used, with also more flexibility in the nozzle sizes and designs. The CW-CRDS spectrometer probing jet-cooled molecules was also updated by using a significantly more reflective set of mirrors in the cavity around the free jet. The performances of the resulting FANTASIO+ set-up were illustrated using various acetylene data. A newly reported sub-band in 2CH, $^{12}C_2H_2$-Ar (K'-K" = 2-3) was presented. Sub-bands of the pure acetylene dimer could be assigned, again in the 2CH excitation range, to *b*- and *a*-type transitions. The latter could possibly correspond to single CH excitation in each of the monomer units.

This report thus definitely assesses the existence of pure acetylene dimers in the 2CH, overtone spectral region. It opens up room for more detailed spectroscopic investigation for both pure and mixed acetylene dimers, and probably of other species relevant for space remote sensing.

Acknowledgements

We are indebted to Dr P. Macko (UK Bratislava) for indicating the commercial availability of the new mirror set we have used, to Dr W.J. Lafferty (NIST) for simulations on larger multimers and to Dr. Colin Western for making his PGOPHER program available. X. de Ghellinck thanks F.R.I.A. for a research grant. We are most indebted to B. Kizil, A. Rizopoulos and P. Van Poucke for their technical help. We thank the Fonds National de la Recherche Scientifique (F.R.S.-FNRS, contracts FRFC and IISN), the Université libre de Bruxelles and the « Action de Recherches Concertées de la Communauté française de Belgique » for financial support.

Figure captions

Figure 1: CW-CRDS jet-cooled spectrum of a mixture of $^{12}C_2H_2$ and Ar around 6548.5 cm^{-1}. The initial FANTASIO set-up was used for the spectrum presented in panel (1), then updated with a second turbomolecular pump in panel (2) then with the more reflective CRDS mirror set in panel (3). The intensity scale was multiplied by a factor 1.5 in panel (3) to reflect the gain in the S/N level, compared to panel (2) (see text). The slit nozzle was 14 X 0.03 mm (1); 30 X 0.015 mm (2); and 10 X 0.03 mm (3). The experimental conditions are 1% C_2H_2 in 99% Ar; p_0/p_∞ = 81000/3.3 Pa (1); 151000/2.1 Pa (2); and 129000/1.6 Pa (3).

Figure 2: Absorption features recorded using FANTASIO+, with $^{12}C_2H_2$ seeded in Ne (top) and Ar (middle) using adapted nozzle geometries. The spectrum of the pure acetylene dimer simulated using *b*-type selection rules is presented at the bottom (see text for further details). The central *Q* branches are identified according to the usual notation $^{\Delta K}\Delta J_{K''}(J'')$. Flow and pressure conditions: C_2H_2/Ne 184/1118 sccm/min, p_0/p_∞ = 322000/0.5 Pa, axisymmetric nozzle, 150 μm diameter (top); C_2H_2/Ar 185/2929 sccm/min, p_0/p_∞ = 126000/2.5 Pa, slit nozzle 10 X 0.03 mm (middle). T_{rot} = 20 K in the simulation.

Figure 3: Portion around 6548 cm^{-1} of the CW-CRDS jet-cooled spectrum of a mixture of $^{12}C_2H_2$ and Ar recorded using the same injection flow rate of Ar and acetylene flow rates increasing in the ratio 1 (bottom), 2 (middle) and 3 (top). The initial FANTASIO spectrometer was used with, however two turbomolecular pumping units. The slit nozzle

was 30 X 0.015 mm. Flow and pressure conditions: C_2H_2/Ar 98.4/4882 sccm/min, p_0/p_∞ = 146000/1.9 Pa (bottom); C_2H_2/Ar 196.8/4882 sccm/min, p_0/p_∞ = 147000/1.6 Pa (middle); C_2H_2/Ar 290/4882 sccm/min, p_0/p_∞ = 149000/1.9 Pa (top).

Figure 4: Portion around 6560 cm^{-1} of the CW-CRDS jet-cooled spectrum of a mixture of $^{12}C_2H_2$ and Ar recorded using the same injection flow rate of Ar and acetylene flow rates increasing in the ratio 1 (bottom), 2 (middle) and 3 (top). The initial FANTASIO spectrometer was used with, however the two turbomolecular pumping units. The slit nozzle was 30 X 0.015 mm. Flow and pressure conditions: C_2H_2/Ar 98.4/4882 sccm/min, p_0/p_∞ = 146000/1.9 Pa (bottom); C_2H_2/Ar 196.8/4882 sccm/min, p_0/p_∞ = 147000/1.6 Pa (middle); C_2H_2/Ar 290/4882 sccm/min, p_0/p_∞ = 149000/1.9 Pa (top).

Figure 5: Bottom: CW-CRDS jet-cooled spectrum of a mixture of $^{12}C_2H_2$ and Ar recorded using FANTASIO+. Top: Spectrum of the pure acetylene dimer simulated using *a*-type selection rules. Middle: Spectrum of the pure acetylene dimer simulated using *a*- and also *b*-type selection rules; The *b*-type $\Delta K = -1$ sub-bands with K" = 3 to 5 are included. The branches are identified according to the usual notation ${}^{\Delta K}\Delta J_{K"}(J")$. Flow and pressure conditions are identical to those of Figure 2 (mid panel). T_{rot} = 20 K in the simulations.

Figure 6: T-shaped structure of the pure acetylene dimer, with principal axes of inertia.

Table legends

Table 1: Positions (cm^{-1}) of the acetylene dimer Q branches observed in the 2CH spectral excitation range. The sub-bands are identified according to the usual notation ${}^{\Delta K}\Delta J_{K''}(J'')$.

Table 2: Constants used to simulate spectral structures attributed to $(^{12}C_2H_2)_2$ in the NIR spectral range.

[a] adapted from Fraser et al.[11] (see text).

References

[1] D. McIntosh, J. Phys. Chem. **11**, 306 (1907).

[2] D. F. Eggers, N. W. Gregory, G. D. Halsey, and B. S. Rabinovitch, *Physical chemistry*. (John Wiley and Sons, 1964).

[3] K. Sakai, A. Kiode, and T. Kihara, Chem. Phys. Lett. **47**, 416 (1977).

[4] T. Aoyama, O. Matsuoka, and N. Nakagawa, Chem. Phys. Lett. **67**, 508 (1979).

[5] D. M. Hoffman, R. Hoffmann, and C. R. Fisel, J. Am. Chem. Soc. **104**, 1858 (1982).

[6] R. D. Pendley and G. E. Ewing, J. Chem. Phys. **78**, 3531 (1983).

[7] R. E. Miller, P. F. Vohralik, and R. O. Watts, J. Chem. Phys. **80**, 5453 (1984).

[8] G. Fischer, R. E. Miller, P. F. Vohralik, and R. O. Watts, J. Chem. Phys. **83**, 1471 (1985).

[9] D. G. Prichard, J. S. Muenter, and B. J. Howard, Chem. Phys. Lett. **135**, 9 (1987).

[10] I. L. Alberts, T. W. Rowlands, and N. C. Handy, J. Chem. Phys. **88**, 3811 (1988).

[11] G. T. Fraser, R. D. Suenram, F. J. Lovas, A. S. Pine, J. T. Hougen, W. J. Lafferty, and J. S. Muenter, J. Chem. Phys. **89**, 6028 (1988).

[12] A. Weber, J. Chem. Phys. **88**, 3428 (1988).

[13] Y. Oshima, Y. Matsumoto, and M. Takami, Chem. Phys. Lett. **147**, 1 (1988).

[14] G. W. Bryant, D. F. Eggers, and R. O. Watts, J. Chem. Soc. Faraday Trans. II **84**, 1443 (1988).

[15] D. G. Prichard, R. N. Nandi, and J. S. Muenter, J. Chem. Phys. **89**, 115 (1988).

[16] R. G. A. Bone, R. D. Amos, and N. C. Handy, Journal of the Chemical Society, Faraday Transactions **86**, 1931 (1990).

[17] J. Yu, S. Su, and J. E. Bloor, J. Chem. Phys. **94**, 5589 (1990).

[18] T. Dunder and R. E. Miller, J. Chem. Phys. **93**, 3693 (1990).

[19] K. Matsumura, F. J. Lovas, and R. D. Suenram, J. Mol. Spectrosc. **150**, 576 (1991).

[20] A. J. Colussi, S. P. Sander, and R. R. Friedl, Chem. Phys. Lett. **178**, 497 (1991).

[21] R. G. A. Bone, T. W. Rowlands, N. C. Handy, and A. J. Stone, Molecular ¨Physics **72**, 33 (1991).

[22] I. I. Suni and W. Klemperer, J. Chem. Phys. **98**, 988 (1993).

[23] J. D. Augspurger and C. E. Dykstra, Int. J. Quantum Chem. **43**, 135 (1992).

[24] R. L. Bhattacharjee, J. S. Muenter, and L. H. Coudert, Journal of Chemical Physics **97**, 8850 (1992).

[25] J. A. Booze and T. Baer, J. Chem. Phys. **98**, 186 (1993).

[26] Y. F. Zhu, S. L. Allman, R. C. Phillips, W. R. Garrett, and C. H. Chen, Chem. Phys. Lett. **224**, 7 (1994).

[27] V. Brenner, P. Millie, and P. Millie, Z. Phys. D **30**, 327 (1994).

[28] S. M. Resende and W. B. De Almeida, Chem. Phys. **206**, 1 (1996).

[29] A. Karpfen, J. Phys Chem. A **103**, 11431 (1999).

[30] K. Shuler and C. E. Dykstra, J. Phys Chem. A **104**, 4562 (2000).

[31] K. Shuler and C. E. Dykstra, J. Phys Chem. A **104**, 11522 (2000).

[32] S. Hirabayashi, N. Yazawa, and Y. Hirahara, J. Phys Chem. A **107**, 4829 (2003).

[33] J. B. Klauda, S. L. Garrison, J. Jiang, G. Arora, and S. I. Sandler, J. Phys Chem. A **108**, 107 (2004).

[34] K. De Bleecker, A. Bogaerts, and W. Goedheer, Physical Review E **73**, 026405 (2006).

[35] Y.-C. Lee, V. Venkatesan, Y.-P. Lee, P. Macko, K. Didriche, and M. Herman, Chem. Phys. Lett. **435**, 247 (2007).

[36] C. C. Wang, P. Zielke, O. F. Sigurbjo¨rnsson, C. Ricardo Viteri, and R. Signorell, J. Phys. Chem. A **113**, 11129 (2009).

[37] A. P. Milce, D. E. Heard, R. E. Miller, and B. J. Orr, Chem. Phys. Lett. **250**, 95 (1996).

[38] C. Lauzin, K. Didriche, P. Macko, J. Demaison, J. Liévin, and M. Herman, J. Phys Chem. A **113**, 2359 (2009).

[39] C. Lauzin, K. Didriche, J. Liévin, M. Herman, and A. Perrin, J. Chem. Phys. **130**, 204306 (2009).

[40] K. Didriche, C. Lauzin, P. Macko, M. Herman, and W. J. Lafferty, Chem. Phys. Lett. **469**, 35 (2009).

[41] K. A. Keppler, G. C. Mellau, S. Klee, B. P. Winnewisser, M. Winnewisser, J. Plíva, and K. N. Rao, J. Mol. Spectrosc. **175**, 411 (1996).

[42] S. Robert, M. Herman, A. Fayt, A. Campargue, S. Kassi, A. Liu, L. Wang, G. Di Lonardo, and L. Fusina, Mol. Phys. **106**, 2581 (2008).

[43] D. Romanini, A. A. Kachanov, and F. Stoeckel, Chem. Phys. Lett. **270**, 546 (1997).

[44] K. W. Busch and M. A. Busch, *Cavity-Ringdown Spectroscopy*. (American Chemical Society, Washington, 1999).

[45] G. Berden, R. Peeters, and G. Meijer, Int. Rev. Phys. Chem. **19**, 565 (2000).

[46] K. Didriche, C. Lauzin, P. Macko, W. J. Lafferty, R. J. Saykally, and M. Herman, Chem. Phys. Lett. **463** 345 (2008).

[47] A. Ramos, J. Santos, L. Abad, D. Bermejo, V. J. Herrero, and I. Tanarro, J. Raman Spectrosc. **40**, 1249 (2009).

[48] M. Herman, K. Didriche, D. Hurtmans, B. Kizil, P. Macko, A. Rizopoulos, and P. Van Poucke, Mol. Phys. **105**, 815 (2007).

[49] D. Romanini, A. A. Kachanov, and F. Stoeckel, Chem. Phys. Lett. **270**, 538 (1997).

[50] P. Macko, D. Romanini, S. N. Mikhailenko, O. V. Naumenko, S. Kassi, A. Jenouvrier, V. G. Tyuterev, and A. Campargue, J. Mol. Spectrosc **227** (227), 90 (2004).

[51] A. E. Thornley and J. M. Hutson, Chem. Phys. Lett. **198**, 1 (1992).

[52] G. T. Fraser, F. J. Lovas, R. D. Suenram, J. Z. Gillies, and C. W. Gillies, Chem. Phys. Lett. **163**, 91 (1992).

[53] PGOPHER, a Program for Simulating Rotational Structure, C.M. Western, University of Bristol, U.K.; http://pgopher.chm.bris.ac.uk

[54] J. Crovisier, Earth, Moon and Planets **79**, 125 (1999).

[55] T. Y. Brooke, A. T. Tokunaga, H. A. Weaver, J. Crovisier, D. Bockelee-Morvan, and D. Crisp, Nature **383**, 606 (1996).

[56] M. J. Mumma, N. Dello Russo, M. A. DiSanti, K. Magee-Sauer, R. E. Novak, S. Brittain, T. Rettig, I. S. McLean, D. C. Reuter, and L.-H. Xu, Science **292**, 1334 (2001).

[57] S. T. Ridgway, Astrophys. J. **187**, L41 (1974).

[58] T. Encrenaz, H. Feuchtgruber, S. K. Atreya, B. Bezard, E. Lellouch, J. Bishop, S. Edgington, T. De Graauw, M. Griffin, and M. F. Kessler, Astron. Astrophys. **333**, L43 (1998).

[59] M. Kanakidou, B. Bonsang, J. C. Le Roulley, G. Lambert, D. Martin, and G. Sennequier, Nature **333**, 51 (1988).

[60] A. Goldman, F. J. Murcray, R. D. Blatherwick, J. R. Gillis, F. S. Bonomo, F. H. Murcray, D. G. Murcray, and R. J. Cicerone, J. Geophys. Res. **86**, 12143 (1981).

[61] A. Coustenis, R. K. Achterberg, B. J. Conrath, D. E. Jennings, A. Marten, D. Gautier, C. A. Nixon, F. M. Flasar, N. A. Teanby, B. Bezard, and e. al, Icarus **189**, 35 (2007).

[62] J. Cernicharo, A. M. Heras, L. B. F. M. Waters, E. Gonzalez-Alfonso, S. Hony, I. Yamamura, M. Guelin, R. Neri, E. Dartois, S. Perez-Martinez, and e. al, European Space Agency, [Special Publication] SP (1999), SP-427(Universe as Seen by ISO, Vol. 1), 285 (1999).

[63] M. Matsuura, P. R. Wood, G. C. Sloan, A. A. Zijlstra, J. T. van Loon, M. A. T. Groenewegen, J. A. D. L. Blommaert, M.-R. L. Cioni, M. W. Feast, H. J. Habing, S. Hony, E. Lagadec, C. Loup, J. W. Menzies, L. B. F. M. Waters, and P. A. Whitelock, Monthly Notices of the Royal Astronomical Society, 415 (2006).

[64] J. P. Fonfria, J. Cernicharo, M. J. Richter, and J. H. Lacy, ApJ **673**, 445 (2008).

[65] J. H. Lacy, N. J. Evans, II, J. M. Achtermann, D. E. Bruce, J. F. Arens, and J. S. Carr, ApJ **342**, L43 (1989).

[66] N. J. Evans, J. H. Lacy, and J. S. Carr, Astrophys. J. **383**, 674 (1991).

[67] F. Lahuis and E. Van Dishoeck, Astron. Astrophys. **355**, 699 (2000).

[68] D. Farrah, J. Bernard-Salas, H. W. W. Spoon, B. T. Soifer, L. Armus, B. Brandl, V. Charmandaris, V. Desai, S. Higdon, D. Devost, and e. al, ApJ **667**, 149 (2007).

[69] P. Sonnentrucker, E. Gonzalez-Alfonso, and D. A. Neufeld, ApJ **671**, L37 (2007).

[70] R. Wehr, S. Kassi, D. Romanini, and L. Gianfrani, Appl. Phys. B **92**, 459 (2008).

[71] G. Durry, J. S. Li, I. Vinogradov, A. Titov, O. Joly, J. Cousin, T. Decarpenterie, N. Amarouche, X. Liu, B. Parvitte, O. Korablev, M. Gerasimov, and V. Zéninari, Appl. Phys. B **DOI 10.1007/s00340-010-3924-y** (2010).

Table 1

a-type	b-type						
${}^{q}Q(J)$	${}^{p}Q_3(J)$	${}^{p}Q_2(J)$	${}^{p}Q_1(J)$	${}^{r}Q_0(J)$	${}^{r}Q_1(J)$	${}^{r}Q_2(J)$	${}^{r}Q_3(J)$
6538.29	6541.80	6544.14	6546.51	6548.84	6551.11	6553.43	6555.70

Table 2

	Ground state [(a)]	**B_2 state**	**A_1 state**
Origin (cm^{-1})	0	6547.58	6538.32
A (MH_Z)	35282	36000	35250
B (MH_Z)	1913.29003	1900	1904
C (MH_Z)	1798.60956	1810	1795
Δ_{JK} (MH_Z)	2.3341	2.3341*	2.3341*

* Constrained to the ground state value.

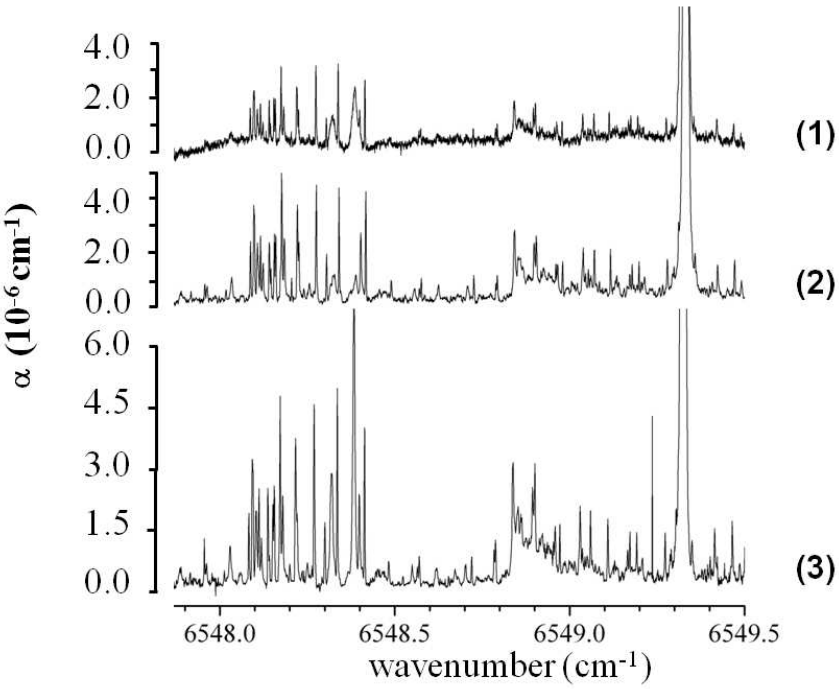

Figure 1: CW-CRDS jet-cooled spectrum of a mixture of 12C2H2 and Ar around 6548.5 cm−1. The initial FANTASIO set-up was used for the spectrum presented in panel (1), then updated with a second turbomolecular pump in panel (2) then with the more reflective CRDS mirror set in panel (3). The intensity scale was multiplied by a factor 1.5 in panel (3) to reflect the gain in the S/N level, compared to panel (2) (see text). The slit nozzle was 14 X 0.03 mm (1); 30 X 0.015 mm (2); and 10 X 0.03 mm (3). The experimental conditions are 1% C2H2 in 99% Ar; p0/p∞ = 81000/3.3 Pa (1); 151000/2.1 Pa (2); and 129000/1.6 Pa (3).
254x190mm (96 x 96 DPI)

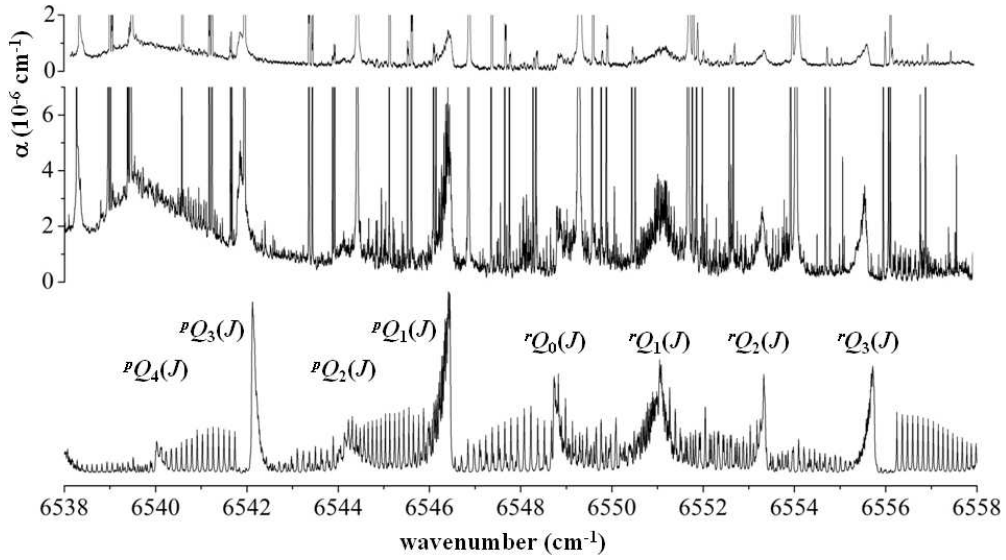

Figure 2: Absorption features recorded using FANTASIO+, with 12C2H2 seeded in Ne (top) and Ar (middle) using adapted nozzle geometries. The spectrum of the pure acetylene dimer simulated using b-type selection rules is presented at the bottom (see text for further details). The central Q branches are identified according to the usual notation . Flow and pressure conditions: C2H2/Ne 184/1118 sccm/min, p0/p∞ = 322000/0.5 Pa, axisymmetric nozzle, 150 μm diameter (top); C2H2/Ar 185/2929 sccm/min, p0/p∞ = 126000/2.5 Pa, slit nozzle 10 X 0.03 mm (middle). Trot = 20 K in the simulation.
254x190mm (96 x 96 DPI)

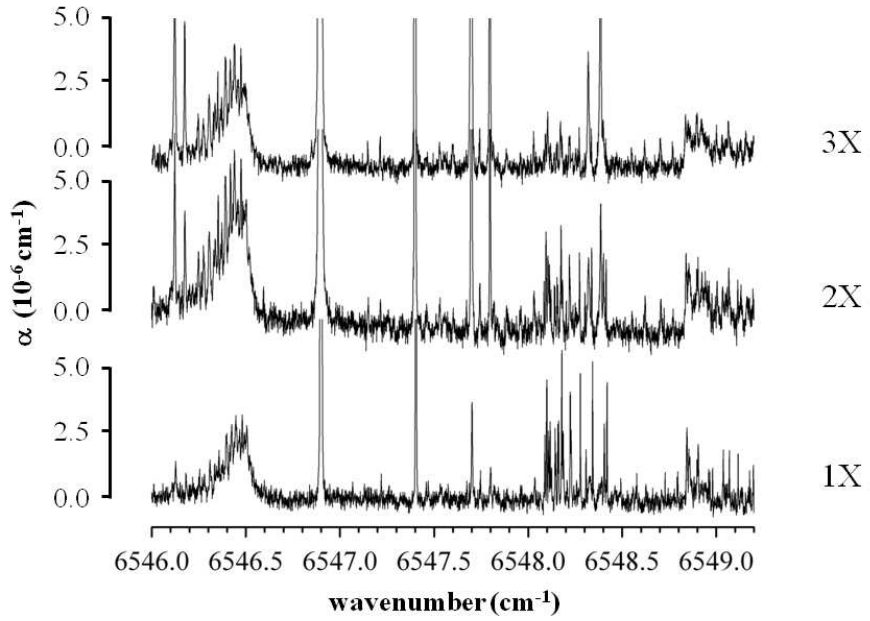

Figure 3: Portion around 6548 cm–1 of the CW-CRDS jet-cooled spectrum of a mixture of 12C2H2 and Ar recorded using the same injection flow rate of Ar and acetylene flow rates increasing in the ratio 1 (bottom), 2 (middle) and 3 (top). The initial FANTASIO spectrometer was used with, however two turbomolecular pumping units. The slit nozzle was 30 X 0.015 mm. Flow and pressure conditions: C2H2/Ar 98.4/4882 sccm/min, p0/p∞ = 146000/1.9 Pa (bottom); C2H2/Ar 196.8/4882 sccm/min, p0/p∞ = 147000/1.6 Pa (middle); C2H2/Ar 290/4882 sccm/min, p0/p∞ = 149000/1.9 Pa (top).
254x190mm (96 x 96 DPI)

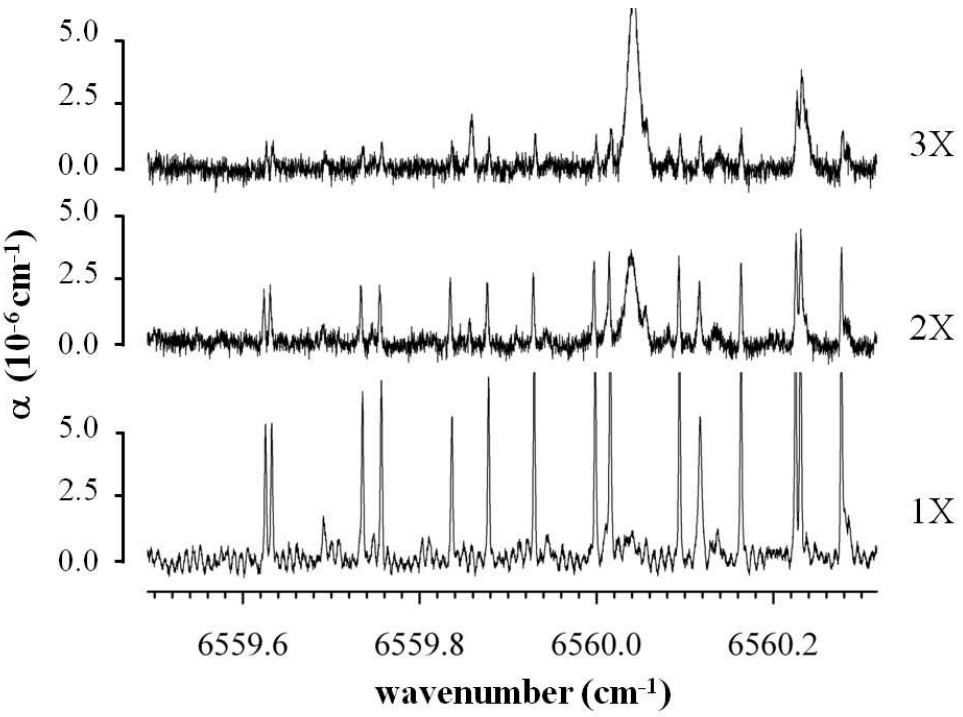

Figure 4: Portion around 6560 cm−1 of the CW-CRDS jet-cooled spectrum of a mixture of 12C2H2 and Ar recorded using the same injection flow rate of Ar and acetylene flow rates increasing in the ratio 1 (bottom), 2 (middle) and 3 (top). The initial FANTASIO spectrometer was used with, however the two turbomolecular pumping units. The slit nozzle was 30 X 0.015 mm. Flow and pressure conditions: C2H2/Ar 98.4/4882 sccm/min, p0/p∞ = 146000/1.9 Pa (bottom); C2H2/Ar 196.8/4882 sccm/min, p0/p∞ = 147000/1.6 Pa (middle); C2H2/Ar 290/4882 sccm/min, p0/p∞ = 149000/1.9 Pa (top).
254x190mm (96 x 96 DPI)

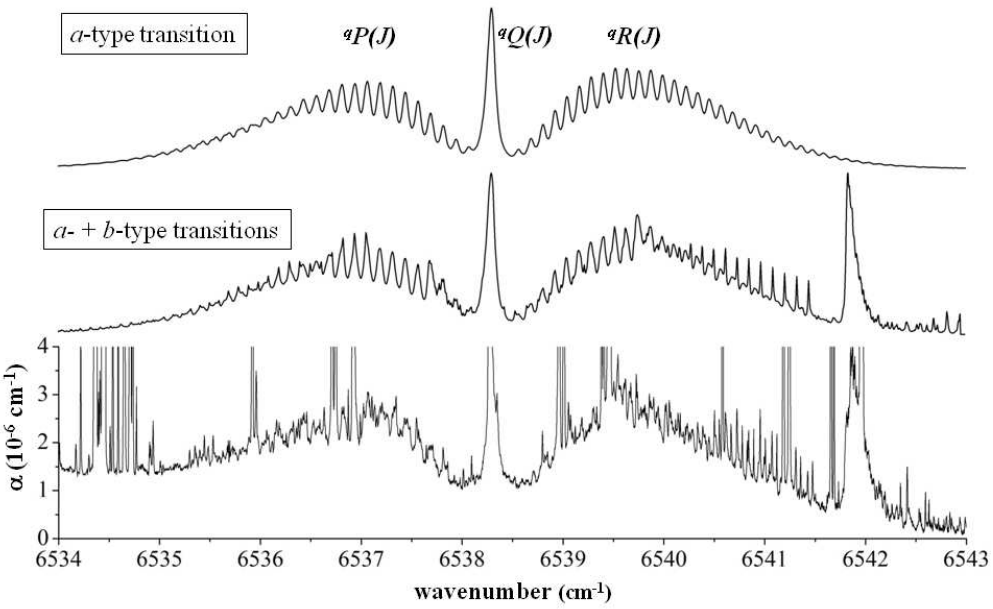

Figure 5: Bottom: CW-CRDS jet-cooled spectrum of a mixture of 12C2H2 and Ar recorded using FANTASIO+. Top: Spectrum of the pure acetylene dimer simulated using a-type selection rules. Middle: Spectrum of the pure acetylene dimer simulated using a- and also b-type selection rules; The b-type sub-bands with K" = 3 to 5 are included. The branches are identified according to the usual notation . Flow and pressure conditions are identical to those of Figure 2 (mid panel). Trot = 20 K in the simulations.
254x190mm (96 x 96 DPI)

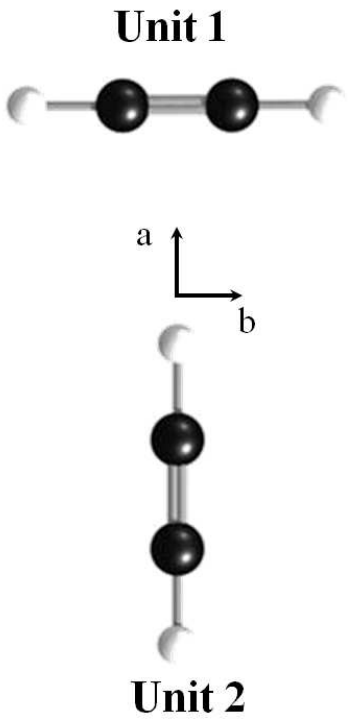

Figure 6: T-shaped structure of the pure acetylene dimer, with principal axes of inertia.
254x190mm (96 x 96 DPI)